PROCEEDINGS A

rspa.royalsocietypublishing.org

Research

Check for updates

Article submitted to journal

Subject Areas:
Complexity, Applied mathematics

Keywords:
Tipping point, Critical transition, Networks, Degree-based mean-field theory

Author for correspondence:
Naoki Masuda
e-mail: naokimas@gmail.com

Mean-field theory for double-well systems on degree-heterogeneous networks

Prosenjit Kundu[1], Neil G. MacLaren[1], Hiroshi Kori[2] and Naoki Masuda[1,3]

[1]Department of Mathematics, State University of New York at Buffalo, NY 14260-2900, USA
[2]Department of Complexity Science and Engineering, The University of Tokyo, Chiba 277-8561, Japan
[3]Computational and Data-Enabled Science and Engineering Program, State University of New York at Buffalo, Buffalo, NY 14260-5030, USA

Many complex dynamical systems in the real world, including ecological, climate, financial, and power-grid systems, often show critical transitions, or tipping points, in which the system's dynamics suddenly transit into a qualitatively different state. In mathematical models, tipping points happen as a control parameter gradually changes and crosses a certain threshold. Tipping elements in such systems may interact with each other as a network, and understanding the behavior of interacting tipping elements is a challenge because of the high dimensionality originating from the network. Here we develop a degree-based mean-field theory for a prototypical double-well system coupled on a network with the aim of understanding coupled tipping dynamics with a low-dimensional description. The method approximates both the onset of the tipping point and the position of equilibria with a reasonable accuracy. Based on the developed theory and numerical simulations, we also provide evidence for multistage tipping point transitions in networks of double-well systems.

THE ROYAL SOCIETY PUBLISHING

1. Introduction

Many empirical complex systems show nonlinear dynamics. Nonlinear behavior sometimes leads to a situation in which the system suddenly shifts from one stable state to a qualitatively, or drastically, different stable state. Reversing such shifts may be difficult due to hysteresis or other reasons. This behavior is widely known as a critical transition or tipping point [1]. Tipping points are observed in a variety of complex dynamical systems including ecological, biological, social, and economical systems. Examples include nutrient-driven shifts in shallow lakes between clear and turbid water [2], abrupt climate changes [3], epileptic seizures [4], and extensive crashes in financial markets [5].

Many tipping point phenomena in nature can be modeled by complex systems that are a collection of tipping elements interacting through a network. Examples include extinction of species in ecosystems in which different species are connected by foodweb, mutualistic, and other ecological networks [6,7], blackouts in power grids [8,9], psychiatric disorders [10,11] and the Greenland ice sheet [12,13]. Obviously, the behavior of the tipping elements is not independent of each other when they are connected as a network [14–16]. For instance, suppose that a tipping element, denoted by v, passes the tipping point, i.e., the value of a control parameter of the system at which a tipping point occurs. Then, it is more likely that a second tipping element directly connected with v will tip as well, resulting in a domino effect [17,18].

Accurately describing the tipping points in dynamics on networks is desirable because we may want to anticipate and prevent them as well as to know the magnitude of a tipping cascade in the network. However, high dimensionality of dynamical systems on a network and the complex structure of the network at hand generally make this task difficult. One strategy towards this goal is to reduce the dimension of the original system without loss of too much information about the original dynamics. For example, Gao, Barzel, and Barabási proposed a theory to reduce a class of dynamical system on networks, including networks of dynamical tipping elements, into one-dimensional dynamics [19]. This method, which we refer to as GBB reduction, is applicable to directed and weighted networks and uses each node's weighted in-degree (i.e., the number of incoming edges) and out-degree (i.e., the number of outgoing edges). The GBB reduction has been generalized to the methods which use the eigenvalues and eigenvectors of the adjacency matrices or related matrices of the network [20–22]. A related but different two-dimensional reduction locates the tipping point with a high accuracy for ecological dynamics occurring on bipartite networks representing mutualistic interactions [23].

The GBB reduction is a degree-based mean-field (DBMF) theory, also called heterogeneous mean-field theory, in the sense that the theory only uses the information about the degree of each node. In general, a DBMF theory for network dynamics assumes that nodes with the same degree are statistically the same and obey the same dynamical rule. It is expected to be accurate for large uncorrelated random networks with general degree distributions. In fact, the most common family of DBMF theory is different from the GBB reduction in that the former aims at deriving a dynamical equation that any node with a given degree obeys, one equation per degree value. In contrast, the goal of the GBB reduction and its extensions is to derive a one-dimensional or low-dimensional reduction of the entire dynamics on the network. To avoid confusion, we save the term DBMF theory only to refer to the conventional type of the DBMF theory and do not refer to the GBB reduction as a DBMF theory below. The DBMF theory (in the conventional sense) has been successful in describing percolation [24–28], dynamic epidemic processes [29–36], synchronization [37–40], random walks [41,42], voter models [43,44], and rock-scissors-paper games [45], to name a few, on degree-heterogeneous uncorrelated networks. A similar DBMF theory for networks of tipping elements, if accurate, will be a useful tool for anticipating tipping points as a system parameter gradually changes and for understanding the impact of the degree distribution on the tipping behavior. Thus motivated, in the present study, we develop a DBMF theory for prototypical dynamical systems showing tipping behavior, i.e., the double-well system, connected as networks.

2. Model

We consider networks in which each node is a tipping element that obeys deterministic dynamics of a double-well system. When there is no interaction between nodes, the state of each node evolves according to

$$\dot{x} = -(x - r_1)(x - r_2)(x - r_3) + u, \tag{2.1}$$

where r_1, r_2, and r_3 are constants (with $r_1 < r_2 < r_3$) and u represents an external input applied to the node. This system has a unique stable equilibrium, x^*, with $x^* < r_1$ when $u < u_{\mathrm{c},\ell}$, where $u_{\mathrm{c},\ell}$ is schematically shown in Fig. 1. We call this equilibrium the lower equilibrium and denote it by x^ℓ. The system has a unique stable equilibrium satisfying $x^* > r_3$, when $u > u_{\mathrm{c,u}}$, where $u_{\mathrm{c,u}}$ is shown in Fig. 1. We call this equilibrium the upper equilibrium and denote it by x^{u}. Both x^ℓ and x^{u} are stable when $u \in (u_{\mathrm{c},\ell}, u_{\mathrm{c,u}})$.

If we initialize the system at the lower equilibrium and gradually increase u, then the system undergoes a saddle-node bifurcation at $u = u_{\mathrm{c,u}}$ such that x^* jumps from the lower equilibrium to the upper equilibrium. If we initialize the system with the upper equilibrium and gradually decrease u, then the system jumps to the lower equilibrium at $u = u_{\mathrm{c},\ell}$, implying a hysteresis. Similar models have been used for representing alternative stable states and hysteresis in ecosystems [46–49], thermohaline circulation [50], and ice sheets [51].

We consider tipping elements that obey the coupled double-well system dynamics given by

$$\dot{x}_i = -(x_i - r_1)(x_i - r_2)(x_i - r_3) + D\sum_{j=1}^{N} A_{ij}x_j + u \quad (i \in \{1, \ldots, N\}), \tag{2.2}$$

where N is the number of nodes, D is the coupling strength, and $A = (A_{ij})$ is the $N \times N$ adjacency matrix of the network. Equation (2.2) has been used for modeling ecological systems such as lake chains in which a node represents a lake [13], global interactions among climate tipping elements such as the Greenland ice sheet, the Atlantic Meridional Overturning Circulation (AMOC), and the Amazon rainforest [49], and Amazon as a network of tipping elements in which each node represents forests within a specific area [47] (also see Refs. [48,52,53] for analyses of the same model). For simplicity, we consider undirected and unweighted networks such that $A_{ij} = A_{ji} \in \{0, 1\}$ for any $i, j \in \{1, \ldots, N\}$. We exclude self-loops, i.e., we set $A_{ii} = 0$ $\forall i \in \{1, \ldots, N\}$. We denote by $k_i = \sum_{j=1}^{N} A_{ij} = \sum_{j=1}^{N} A_{ji}$ the degree of the ith node and by $p(k)$ the degree distribution. This model allows us to investigate tipping cascades on networks.

3. Degree-based mean-field theory

To describe the dynamics given by Eq. (2.2), we develop a DBMF theory, which assumes that the nodes with degree k are statistically equivalent to each other and that the states of different nodes are statistically independent of each other except their dependence on k. This assumption corresponds to a configuration model of networks, i.e., a random network with a given degree sequence or distribution. In this theory, we replace the elements of the adjacency matrix, A_{ij}, by its ensemble average, denoted by $\langle A_{ij} \rangle$, which represents the probability that the ith and jth nodes are adjacent to each other, assuming $\langle A_{ij} \rangle \leq 1$. For uncorrelated networks, we obtain

$$\langle A_{ij} \rangle = \frac{k_i k_j}{N\langle k \rangle}. \tag{3.1}$$

Equation (3.1) implies that the probability that the jth node is a neighbor of an arbitrary node is equal to $k_j / (N\langle k \rangle)$. The DBMF theory based on Eq. (3.1) was first pioneered for percolation and the susceptible-infectious-susceptible model (see Section 1 for references).

By substituting Eq. (3.1) in Eq. (2.2), we obtain

$$\dot{x}_i = -(x_i - r_1)(x_i - r_2)(x_i - r_3) + Dk_i\Theta + u, \tag{3.2}$$

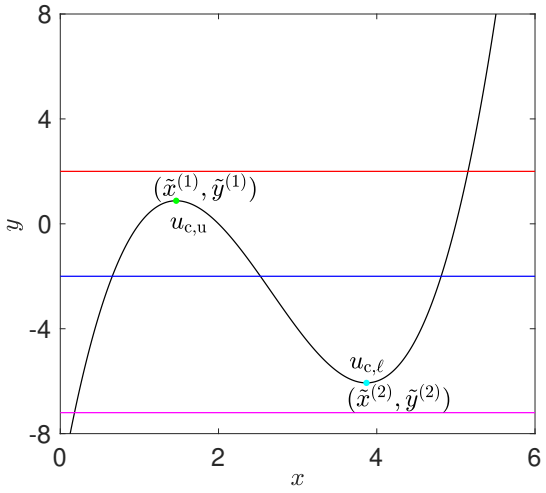

Figure 1. Graphical representation of the equilibria of the single and the coupled double-well systems. Under the DBMF theory, the intersection of $y = (x_i - r_1)(x_i - r_2)(x_i - r_3)$ and $y = Dk_i\Theta + u$ gives x_i at equilibrium.

where

$$\Theta = \frac{1}{N\langle k\rangle}\sum_{j=1}^{N} k_j x_j \tag{3.3}$$

is the degree-weighted average of x_j, and $\langle k\rangle$ is the average degree.

For a given Θ value, the equilibria of Eq. (3.2) is given by the intersection of the cubic polynomial $y = (x_i - r_1)(x_i - r_2)(x_i - r_3)$ and the horizontal line $y = Dk_i\Theta + u$ in the x-y plane (see Fig. 1). Denote by $(\tilde{x}^{(1)}, \tilde{y}^{(1)})$ the unique local maximum of $y = (x - r_1)(x - r_2)(x - r_3)$ and by $(\tilde{x}^{(2)}, \tilde{y}^{(2)})$ the unique local minimum.

For the nodes with the smallest degrees satisfying $Dk_i\Theta + u < \tilde{y}^{(2)}$, the curve $y = (x_i - r_1)(x_i - r_2)(x_i - r_3)$ and the line $y = Dk_i\Theta + u$ have just one intersection at $x_i < \tilde{x}^{(1)}$ such that there is a unique stable equilibrium, which we call the lower state (see the magenta line in Fig. 1). For the nodes with the largest degrees satisfying $Dk_i\Theta + u > \tilde{y}^{(1)}$, there is a unique stable equilibrium satisfying $x_i \geq x^{(2)}$, which we call the upper state (see the red line in Fig. 1). Finally, for the nodes whose degree satisfies $\tilde{y}^{(2)} < Dk_i\Theta + u < \tilde{y}^{(1)}$, Eq. (3.2) allows both lower and upper states (see the blue line in Fig. 1).

We assume that all nodes are initially in their respective lower states and that we gradually increase u. A larger value of $Dk_i\Theta + u$ induces the upper state for the ith node under the DBMF theory. Therefore, at a given value of u, the Nq nodes with the smallest degree, i.e., the nodes whose k_i is smaller than a threshold value $\tilde{k}$, are in the lower state, where q is the fraction of nodes in the lower state. The other $N(1-q)$ nodes, which have $k_i \geq \tilde{k}$, are in the upper state. The value of k_i that satisfies $Dk_i\Theta + u = \tilde{y}^{(1)}$ is equal to $\tilde{k}$. In other words, we obtain

$$\tilde{k} = \frac{\tilde{y}^{(1)} - u}{D\Theta^*}, \tag{3.4}$$

where Θ^* is the Θ value in the equilibrium.

Similar to the analysis of epidemic process models [29–36], we need to self-consistently determine Θ^*. Using Eq. (3.3), we obtain

$$\Theta^* = \frac{1}{N\langle k\rangle}\left[\sum_{k<\tilde{k}} kx^{\ell}(k) + \sum_{k\geq\tilde{k}} kx^{\mathrm{u}}(k)\right], \tag{3.5}$$

where $x^{\ell}(k)$ and $x^{\mathrm{u}}(k)$ are the lower and upper states, respectively, which are functions of k and Θ^*.

We obtain Θ^* and $\tilde{k}$ from Eqs. (3.4) and (3.5) as follows. First, the right-hand side of Eq. (3.5), which we write $\Theta_2^*(\tilde{k})$, is a continuous and monotonically decreasing function of $\tilde{k}$, given the Θ^* value with which to calculate the $x^{\ell}(k)$ or $x^{\mathrm{u}}(k)$ value for each k. We obtain $\lim_{\tilde{k}\to 0}\Theta_2^*(\tilde{k}) = \Theta_2^*(k_{\min}) = \langle kx^{\mathrm{u}}(k)\rangle/\langle k\rangle$ and $\lim_{\tilde{k}\to\infty}\Theta_2^*(\tilde{k}) = \lim_{\tilde{k}\downarrow k_{\max}}\Theta_2^*(\tilde{k}) = \langle kx^{\ell}(k)\rangle/\langle k\rangle$, where $\langle\cdot\rangle$ is the average over the N nodes. Second, we rewrite Eq. (3.4) as $\Theta_1^*(\tilde{k}) \equiv (\tilde{y}^{(1)} - u)/(D\tilde{k})$. It holds true that $\Theta_1^*(\tilde{k})$ is also a continuous and monotonically decreasing function of $\tilde{k}$, $\lim_{\tilde{k}\downarrow 0}\Theta_1^*(\tilde{k}) = \infty$, and $\lim_{\tilde{k}\to\infty}\Theta_1^*(\tilde{k}) = 0$. Because $\lim_{\tilde{k}\downarrow 0}\left[\Theta_1^*(\tilde{k}) - \Theta_2^*(\tilde{k})\right] > 0$ and $\lim_{\tilde{k}\to\infty}\left[\Theta_1^*(\tilde{k}) - \Theta_2^*(\tilde{k})\right] < 0$, there is at least one positive value of $\tilde{k}$ that solves $\Theta_1^*(\tilde{k}) - \Theta_2^*(\tilde{k}) = 0$, which one can obtain by, for example, the bisection method. Although there may be multiple roots of $\Theta_1^*(\tilde{k}) - \Theta_2^*(\tilde{k}) = 0$ depending on the degree distribution, with a practical degree distribution, $\Theta_1^*(\tilde{k}) - \Theta_2^*(\tilde{k}) = 0$ usually has only one root. We regard that all the nodes are in the upper or lower states if the obtained solution satisfies $\tilde{k} \le k_{\min}$ or $\tilde{k} > k_{\max}$, respectively.

4. Numerical results

In this section, we mainly investigate the accuracy of the DBMF theory developed in Section 3 against direct numerical simulations in locating the tipping point and approximating $\{x_1, \ldots, x_N\}$ at equilibrium.

(a) Numerical methods and networks

We set $r_1 = 1$, $r_2 = 2$, and $r_3 = 5$. We either fix D and vary u (Section 4(b)) or fix u and vary D (Section 4(c)). For the given u and D values, we set the initial conditions to $x_i = 0.01$ (with $i = 1, \ldots, N$) and run simulations for 30000 time units to ensure that the equilibrium has been reached. At a relatively small value of u or D, all the nodes are in their lower state at equilibrium. Then, we gradually increase u or D.

We use the following networks. First, we use networks generated by the Barabási-Albert (BA) model [54] that produces scale-free networks with $p(k) \propto k^{-3}$, where $\propto$ represents "proportional to". We refer to these networks as BA networks. To generate a BA network, we start with a network with two nodes connected by an edge and connect each of the two edges emanating from each new node to an existing node according to the linear preferential attachment rule. We obtain $\langle k\rangle \approx 4$, where $\approx$ represents "approximately equal to".

Second, we use the Holme-Kim network model [55], which is a modification of the BA model for high clustering (i.e., a large number of triangles). We construct networks with average degree $\langle k\rangle \approx 10$ by setting the number of edges that each new node brings in to five. We set the probability of constructing a triangle for the each new edge to 0.5. Third, we use the largest connected component (LCC) of a coauthorship network of researchers in network science, which has $N = 379$ nodes and 914 undirected edges [56]. Each node in this network represents a researcher publishing a paper in network science up to year 2006. An edge exists between two nodes if the two researchers coauthored at least one paper. Finally, we use the LCC of the hamsterster social network, which has $N = 1788$ nodes and 12476 undirected edges [57]. A node in this network represents a user of hamsterster.com. Two users are adjacent if they have a friendship relation on the website.

We compare the performance of the DBMF theory with that of the GBB reduction. The GBB reduction for the coupled double-well system (see Eq. (2.2)) is given by

$$\dot{x} = -(x - r_1)(x - r_2)(x - r_3) + D\beta x + u, \tag{4.1}$$

where $\beta = \sum_{i=1}^{N} k_i^2 / \sum_{i=1}^{N} k_i$ [19]. When the GBB reduction is accurate, the dynamics and equilibria of x obtained from Eq. (4.1) closely approximate those of the observable x_{eff}, called

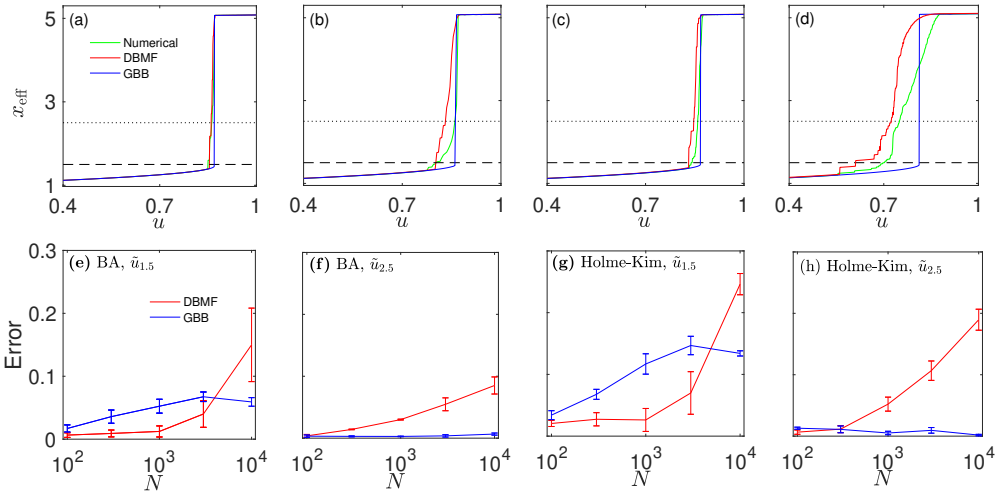

Figure 2. Performance of the DBMF theory and GBB reduction on approximating the effective state, $x_{\rm eff}$, in different networks when we set $D = 0.001$ and vary u. (a) BA network with $N = 10^2$ nodes. (b) BA network with $N = 10^3$ nodes. (c) Coauthorship network. (d) Hamsterster network. (e) Approximation error for the DBMF theory and GBB reduction in locating the tipping point, $\tilde{u}_{1.5}$, for BA networks with different numbers of nodes. (f) Approximation error in locating $\tilde{u}_{2.5}$ for BA networks. (g) Approximation error in locating $\tilde{u}_{1.5}$ for Holme-Kim networks. (h) Approximation error in locating $\tilde{u}_{2.5}$ for Holme-Kim networks. In (a)–(d), the dashed and dotted lines represent $x_{\rm eff} = 1.5$ and $x_{\rm eff} = 2.5$, respectively. In (e)–(h), the error bars represent the average $\pm$ standard deviation calculated on the basis of 100 simulations, each of which uses a different network instance with the given number of nodes.

the effective state, given by

$$x_{\rm eff} = \frac{\sum_{i=1}^{N} k_i x_i}{\sum_{i=1}^{N} k_i}, \tag{4.2}$$

where we obtain $\{x_1, \ldots, x_N\}$ from direct numerical simulations of the original N-dimensional dynamical system, Eq. (2.2). To compare the accuracy of the DBMF theory with the GBB, we measure the effective state calculated from the DBMF theory given by

$$x_{\rm DBMF} = \frac{\sum_{k=k_{\rm min}}^{k_{\rm max}} k x(k)}{\sum_{k=k_{\rm min}}^{k_{\rm max}} k}, \tag{4.3}$$

where $x(k)$ is either $x^{\ell}(k)$ or $x^{\rm u}(k)$.

(b) Tipping under gradual increases in u

We set $D = 0.001$ and vary u in this section. We show the dependence of $x_{\rm eff}$ on u for a BA network with $N = 10^2$ nodes, a BA network with $N = 10^3$ nodes, the coauthorship network, and the hamsterster network in Figs. 2(a), 2(b), 2(c), and 2(d), respectively. We find that, in numerical simulations, the tipping point does not occur at the same value of u for the different nodes, resulting in gradual transitions from the lower state to the upper state as one increases u; we will examine this phenomenon in Section 4(d) . Therefore, we need to define which tipping points we want to anticipate by theory. Because we are usually interested in critical points at which a macroscopic number of nodes (i.e., $O(N)$) starts to experience a major transition, we operationally define the tipping point as the value of u at which $x_{\rm eff}$ exceeds 1.5, denoted by $\tilde{u}_{1.5}$ (see the dashed lines in Fig. 2) for the first time as we gradually increase u. Roughly speaking, 5–10% of the nodes have switched from the lower state to the upper state at $u = \tilde{u}_{1.5}$. Figures 2(a)–(d) suggest that the

DBMF theory better approximates $\tilde{u}_{1.5}$ than the GBB reduction does. We quantitatively confirm this claim in Table 1, which compares the error in the tipping point defined by $|u_{\rm GBB} - \tilde{u}_{1.5}|$ for GBB reduction and $|u_{\rm DBMF} - \tilde{u}_{1.5}|$ for our DBMF theory, where $u_{\rm GBB}$ and $u_{\rm DBMF}$ are the tipping point estimated by the GBB reduction and the DBMF theory, respectively. We note that we do not add a generalization of the GBB reduction [20,21] to the present comparison because the DBMF theory and the GBB reduction only use the degree of each node, whereas the generalizations of the GBB reduction use the full adjacency matrix of the network [22].

The accuracy of the different approximations depends on the definition of the tipping point. To show this, consider a tipping point defined as the value of u at which $x_{\rm eff}$ exceeds 2.5 for the first time as one increases u, denoted by $\tilde{u}_{2.5}$ (see the dotted lines in Fig. 2). With this definition, the DBMF theory is better at locating the tipping point than the GBB reduction for two networks and vice versa for the other two networks (see Table 1).

We also confirmed that, for BA networks of different sizes, the error in locating the tipping point is systematically smaller for the DBMF theory than the GBB reduction when we use $\tilde{u}_{1.5}$ as the tipping point (see Fig. 2(e)), whereas the opposite is the case with $\tilde{u}_{2.5}$ (see Fig. 2(f)). With both $\tilde{u}_{1.5}$ and $\tilde{u}_{2.5}$, the error increases as N increases.

We show the approximation error for the GBB reduction and the DBMF theory for Holme-Kim networks in Figs. 2(g) and 2(h) for $\tilde{u}_{1.5}$ and $\tilde{u}_{2.5}$, respectively. The results are similar to the case of BA networks (see Figs. 2(e) and 2(f)) despite the presence of high clustering in the Holme-Kim networks. Specifically, the DBMF theory is better approximating the tipping point than the GBB reduction for the tipping point $\tilde{u}_{1.5}$ (see Fig. 2(g)), whereas the opposite holds true except for small networks in the case of $\tilde{u}_{2.5}$ (see Fig. 2(h)).

Table 1. Approximation error for the DBMF theory and GBB reduction. We set $D = 0.001$ and gradually increase u to determine tipping points $\tilde{u}_{1.5}$ and $\tilde{u}_{2.5}$. We set $u = 0$ and gradually increase D to determine tipping points $\tilde{D}_{1.5}$ and $\tilde{D}_{2.5}$.

	$\tilde{u}_{1.5}$		$\tilde{u}_{2.5}$		$\tilde{D}_{1.5}$		$\tilde{D}_{2.5}$	
Network	DBMF	GBB	DBMF	GBB	DBMF	GBB	DBMF	GBB
BA, $N = 10^2$	0.004	0.014	0.002	0.007	0.007	0.048	0.001	0.031
BA, $N = 10^3$	0.002	0.053	0.026	0.002	0.012	0.034	0.023	0.007
Coauthorship	0.008	0.027	0.012	0.008	0.009	0.043	0.012	0.029
Hamsterter	0.092	0.109	0.025	0.063	0.001	0.007	0.001	0.005

We next compared the performance of the DBMF theory and the GBB reduction in approximating the the effective state, $x_{\rm eff}$, off the tipping point, which has been a main goal of recent papers on dimension reduction techniques for dynamical systems on networks [19–21,58–60]. To quantify the accuracy at approximating $x_{\rm eff}$, we measure the relative error between the results obtained from direct numerical simulations and the theoretical estimate, which we denote by ϵ. For the DBMF theory, we obtain $\epsilon = |(x_{\rm eff} - x_{\rm DBMF})/x_{\rm eff}|$, where $x_{\rm eff}$ refers to the value obtained from direct numerical simulations. For the GBB reduction, we set $\epsilon = |(x_{\rm eff} - x(\beta))/x_{\rm eff}|$, where we obtain $x(\beta)$ as the equilibrium of the one-dimensional dynamics given by Eq. (4.1). At each u value, we calculate the average and standard deviation of the relative error on the basis of 100 BA networks. We show the relative error for BA networks with $N = 10^2$ and $N = 10^3$ nodes in Figs. 3(a) and 3(b), respectively, for a range of u above the tipping point. The relative error for the DBMF theory is similar to that for the GBB reduction when $N = 10^2$. The GBB reduction yields smaller errors when $N = 10^3$. However, the relative error for the DBMF theory when $N = 10^3$ is also fairly small (i.e., $< 0.5 \times 10^{-3}$). We show in Fig. 3(c) the mean and standard deviation of the relative error at $u = 1.5$ as a function of N. Although the error for the DBMF theory increases as N increases, it remains reasonably small up to $N = 10^4$.

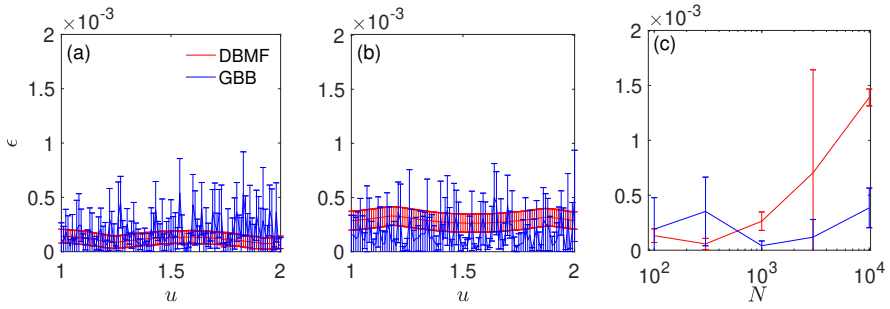

Figure 3. Relative error in approximating the effective state by the DBMF theory and GBB reduction. We use BA networks with N nodes. (a) $N = 100$. (b) $N = 1000$. (c) Dependence on N at $u = 1.5$. In (a) and (b), we omitted the part of the error bar below $\epsilon = 0$.

(c) Tipping under gradual increases in D

Next, we examine the accuracy of the DBMF theory and GBB reduction when we set $u = 0$ and vary D. In Fig. 4(a), (b), (c), and (d), we show the relationship between $x_{\rm eff}$ and D for a BA network with $N = 10^2$ nodes, a BA network with $N = 10^3$ nodes, the coauthorship network, and the hamsterster network, respectively. For approximating the location of the tipping point, we find that our DBMF theory is more accurate than the GBB reduction when we define the tipping point by $\tilde{D}_{1.5}$, i.e, the value of D at which $x_{\rm eff}$ exceeds 1.5 for the first time when we increase the value of D (see the dashed lines in Fig. 4). If we define the tipping point by $\tilde{D}_{2.5}$ (see the dotted lines in Fig. 4), the DBMF theory is more accurate on the BA network with $N = 10^2$ nodes (Fig. 4(a)) and the hamsterster network (Fig. 4(d)) and vice versa on the BA network with $N = 10^3$ nodes (Fig. 4(b)) and the coauthourship network (Fig. 4(c)); also see Table 1.

With BA networks with different numbers of nodes, the DBMF theory locates $\tilde{D}_{1.5}$ more accurately than the GBB reduction (see Fig. 4(e)). The opposite is the case when we define the tipping point by $\tilde{D}_{2.5}$ (see Fig. 4(f)) except for small networks.

We also show the error in approximating the tipping point for Holme-Kim networks with different numbers of nodes in Figs. 4(g) and 4(h). The DBMF theory locates the tipping point with a higher accuracy than the GBB reduction with the tipping point being defined by $\tilde{D}_{1.5}$ (Fig. 4(g)), whereas the opposite is the case for the combination of $\tilde{D}_{2.5}$ and large N (Fig. 4(h)). All these results are similar to those when we varied u instead of D (see Section 4(b)).

(d) Multistage transitions

For the given D value, the DBMF theory predicts a range of parameter value $u \in (u_{\rm c,\ell}, u_{\rm c,u})$ over which the different nodes tip from the lower to the upper state. Using Eq. (3.2) and Fig. 1, we obtain

$$u_{\rm c,\ell} = \tilde{y}^{(2)} - Dk_{\rm max}\Theta^* \tag{4.4}$$

and

$$u_{\rm c,u} = \tilde{y}^{(1)} - Dk_{\rm min}\Theta^*. \tag{4.5}$$

Therefore, except for regular networks (i.e., those in which all nodes have the same degree), one obtains $u_{\rm c,\ell} < u_{\rm c,u}$ such that there is a nonvanishing range of u in which some nodes are in the lower state and the other nodes are in the upper state. Therefore, the entire N-dimensional dynamical system on the network does not show a single tipping point but undergoes multiple tipping points in uncorrelated degree-heterogeneous networks even when $N \to \infty$. We refer to this phenomenon as multistage transition. Equations (4.4) and (4.5) indicate that the range of u through which a multistage transition occurs is wider for a more heterogeneous degree

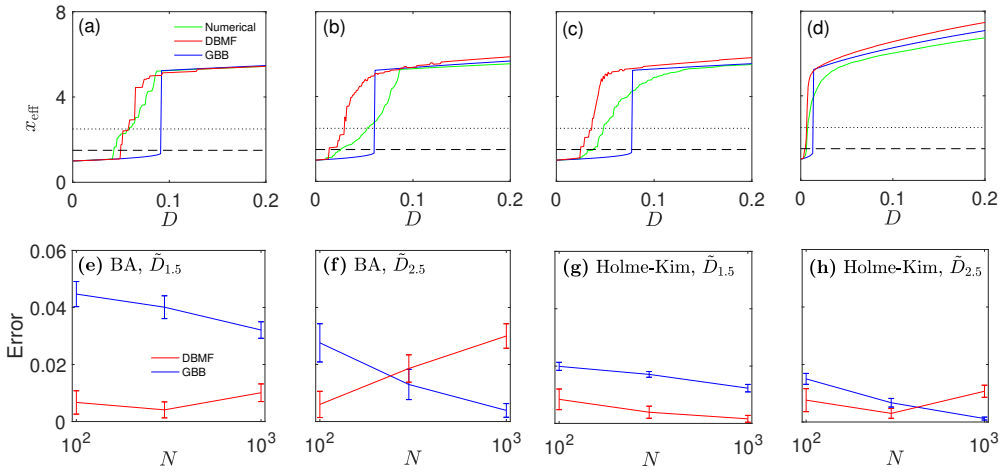

Figure 4. Performance of the DBMF theory and GBB reduction on approximating the effective state, $x_{\rm eff}$, in different networks when we set $u = 0$ and vary D. (a) BA network with $N = 10^2$ nodes. (b) BA network with $N = 10^3$ nodes. (c) Coauthorship network. (d) Hamsterster network. (e) Approximation error for the DBMF theory and GBB reduction in locating the tipping point, $\tilde{D}_{1.5}$, for BA networks. (f) Approximation error in locating $\tilde{D}_{2.5}$ for BA networks. (g) Approximation error in locating $\tilde{D}_{1.5}$ for Holme-Kim networks. (h) Approximation error in locating $\tilde{D}_{2.5}$ for Holme-Kim networks. In (a)–(d), the dashed and dotted lines represent $x_{\rm eff} = 1.5$ and $x_{\rm eff} = 2.5$, respectively. See the caption of Fig. 2 for the definition of the error bar.

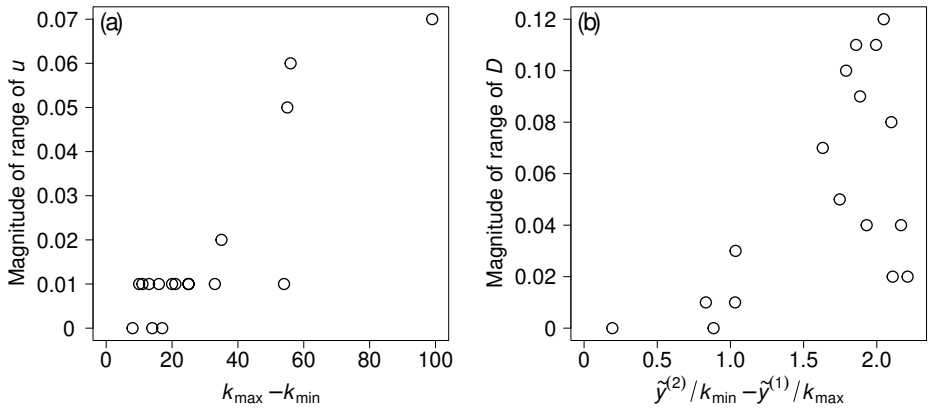

Figure 5. The relationship between the degree heterogeneity and the range of a bifurcation parameter over which multiple transitions occur. In (a), we fix $D = 0.001$ and gradually increase u. In (b), we fix $u = 0$ and gradually increase D. A circle represents a network. We gathered networks from [61] which originated in published research [62–78].

distribution. Similarly, when one fixes u and varies D, a multistage transition occurs over $D \in \left((u - \tilde{y}^{(2)})/k_{\rm max}, (u - \tilde{y}^{(1)})/k_{\rm min}\right)$.

To verify this prediction, we numerically simulated double-well dynamics on several networks. We selected 17 networks from the archive of empirical networks in the "networkdata" R package [61] that were a mix of human and animal social networks with between 34 and 379 nodes (and mean $= 116.2$). We simplified the networks by making them undirected and unweighted, retaining only the largest connected component, and allowing no self-loops. When

several networks drawn from a published work were available, we used a network with close to 100 nodes. We kept increasing the bifurcation parameter (i.e., u or D) until at least 90% of nodes were in the upper state at equilibrium. Then, we calculated the range of the bifurcation parameter over which node transitions occurred as the difference between the first value when at least 10% of nodes were in the upper state and the first value when at least 90% of nodes were in the upper state.

In Fig. 5(a), we show the relationship between the observed range of u and the range of node degrees (i.e., $k_{\max} - k_{\min}$) for each network when we fix $D = 0.001$ and vary u. Each circle represents a network. Equations (4.4) and (4.5) imply that the size of the range of u is proportional to $k_{\max} - k_{\min}$, which the results shown in Fig. 5(a) supports. The Pearson correlation coefficient between the size of the range of u and $k_{\max} - k_{\min}$ is 0.87. In Fig. 5(b), we show the relationship between the range of D over which multiple transitions occur and $\tilde{y}^{(2)}/k_{\min} - \tilde{y}^{(1)}/k_{\max}$ when we fix $u = 0$ and vary D. Note that $D \in \left((u - \tilde{y}^{(2)})/k_{\max}, (u - \tilde{y}^{(1)})/k_{\min}\right)$ implies that the size of the range of D is proportional to $\tilde{y}^{(2)}/k_{\min} - \tilde{y}^{(1)}/k_{\max}$. Figure 5(b) is also supportive of the DBMF theory; the Pearson correlation coefficient between the two quantities is 0.59. In both cases, the heterogeneity in the degree distribution in terms of $k_{\min}$ and $k_{\max}$ predicts the presence of multistage transitions fairly well.

5. Discussion

We have developed a DBMF theory for a standard double-well system on networks. The DBMF theory has turned out to be more accurate than the GBB reduction in locating the tipping point if we define it as the bifurcation parameter value at which a small fraction of nodes has tipped. We have also shown that the DBMF theory is less accurate than the GBB reduction at approximating the effective state substantially above the tipping point.

The original spectral method is a generalization of the GBB reduction and uses the leading eigenvector of the adjacency matrix to linearly combine $\{x_1, \ldots, x_N\}$ and realize a low-dimensional reduction of a family of dynamical systems on networks [20,21]. Similar to the GBB reduction, the original spectral method is accurate at approximating the effective state, whereas it is not accurate at locating the tipping point [60]. We recently extended this spectral method to the case of the nonleading eigenvector that minimizes a mathematically derived error [22]. By design, this spectral method, which we call the modified spectral method, is more accurate than the original spectral method, and presumably than the GBB reduction and DBMF theory, at approximating the effective state except near the tipping point. However, the modified spectral method is far less accurate at locating the tipping point than the original spectral method, and also apparently than the GBB reduction and DBMF theory [22]. Therefore, it seems that the accuracy at locating the tipping point and that at approximating the effective state sufficiently far from the tipping point are in a trade-off relationship. Specifically, among the methods discussed here, the DBMF theory is the most accurate at the former task, the modified spectral method is the most accurate at the latter task, and the GBB and the original spectral method are in between. Looking more closely into this trade-off, including searching a theory that more accurately locates the tipping point than the present DBMF theory, warrants future work.

There exists a critical value of the parameter at which the lower and upper equilibrium states have the same potential energy and thus have the same resilience [79,80]. In this case, there exists the tipping point at which half nodes belong to the lower equilibrium and the other half to the upper equilibrium. With this definition of the tipping point, i.e., $u = u_{2.5}$ or $D = D_{2.5}$ in our case, we have shown that our DBMF theory is not accurate. In the present study, our primary definition of the tipping point is the value of the parameter at which a small fraction of nodes (5–10%) has transitioned from the lower to upper state (i.e., $u = u_{1.5}$ or $D = D_{1.5}$). We chose such a small fraction because, in practice, we are often interested in the situation in which a small but noticeable fraction of nodes, rather than half the nodes, has tipped to enter an undesirable state. For example, the tipping point for the flip to non-forest ecosystems in eastern, southern and

central Amazonia is estimated to be at 20–25% deforestation [81]. We have shown that our DBMF theory is more accurate than the GBB reduction with this latter definition of tipping.

In the present study, we have assumed that the influence of the jth node on the ith node is proportional to $A_{ij}x_j$, where A_{ij} is the (i,j) element of the adjacency matrix. In contrast, double-well systems on networks in which the nodes are diffusively coupled have also been studied. Such a model represents, for example, chemical reaction diffusion [82–84]. A DBMF theory was previously developed for the case of diffusive coupling [82]. However, adapting their theory to be able to self-consistently determine the mean field (i.e., Θ^* in our formulation) and the threshold degree (i.e., $\tilde{k}$), and thus further pursuing how nodes with different degrees behave and comparing the results with the case of coupling by the adjacency matrix warrants future work.

We have provided theoretical and numerical evidence of multistage transitions in the present double-well system on networks. In particular, our DBMF theory suggests that the multistage transition is not a finite-size effect because the DBMF theory is more accurate in large uncorrelated networks in general. In fact, our DBMF theory depends on the number of nodes, N, through Eq. (3.5). However, an increase in N does not mitigate the validity of Eqs. (4.4) and (4.5), which suggests that multistage transitions are likely to occur in networks of different sizes. Investigating multistage transitions for a wider variety of networks and dynamical systems, as well as their practical implications, also warrants future work.

Data Accessibility. The empirical networks used in this paper are found in Refs. [56,57,61–78].

Authors' Contributions. N.M. and H.K. conceived the research. N.M. developed the theory. P.K. and N.G.M. performed the numerical analysis. P.K., N.G.M., H.K., and N.M. discussed the results and wrote the paper.

Competing Interests. Authors declare that they have no competing interests.

Funding. H.K. acknowledges support from JSPS KAKENHI under Grant No. 21K12056. N.M. acknowledges support from AFOSR European Office (under Grant No. FA9550-19-1- 7024), the Sumitomo Foundation, the Japan Science and Technology Agency (JST) Moonshot R&D (under Grant No. JPMJMS2021), and the National Science Foundation (under Grant No. 2052720).

References

1. Scheffer M. 2009 *Critical Transitions in Nature and Society*. Princeton University Press.
2. Carpenter SR, Cole JJ, Pace ML, Batt R, Brock WA, Cline T, Coloso J, Hodgson JR, Kitchell JF, Seekell DA et al.. 2011 Early warnings of regime shifts: a whole-ecosystem experiment. *Science* **332**, 1079–1082.
3. Lenton TM, Held H, Kriegler E, Hall JW, Lucht W, Rahmstorf S, Schellnhuber HJ. 2008 Tipping elements in the Earth's climate system. *Proc. Natl. Acad. Sci. USA* **105**, 1786–1793.
4. Litt B, Esteller R, Echauz J, D'Alessandro M, Shor R, Henry T, Pennell P, Epstein C, Bakay R, Dichter M et al.. 2001 Epileptic seizures may begin hours in advance of clinical onset: a report of five patients. *Neuron* **30**, 51–64.
5. May RM, Levin SA, Sugihara G. 2008 Ecology for bankers. *Nature* **451**, 893–894.
6. Allesina S, Tang S. 2012 Stability criteria for complex ecosystems. *Nature* **483**, 205–208.
7. Grilli J, Adorisio M, Suweis S, Barabás G, Banavar JR, Allesina S, Maritan A. 2017 Feasibility and coexistence of large ecological communities. *Nat. Commun.* **8**, 14389.
8. Carreras BA, Lynch VE, Dobson I, Newman DE. 2002 Critical points and transitions in an electric power transmission model for cascading failure blackouts. *Chaos* **12**, 985–994.
9. Dobson I, Carreras BA, Lynch VE, Newman DE. 2007 Complex systems analysis of series of blackouts: Cascading failure, critical points, and self-organization. *Chaos* **17**, 026103.
10. Hayes AM, Yasinski C, Barnes JB, Bockting CL. 2015 Network destabilization and transition in depression: New methods for studying the dynamics of therapeutic change. *Clin. Psychol. Rev.* **41**, 27–39.
11. Cramer AO, Van Borkulo CD, Giltay EJ, Van Der Maas HL, Kendler KS, Scheffer M, Borsboom D. 2016 Major depression as a complex dynamic system. *PLoS ONE* **11**, e0167490.

12. Kriegler E, Hall JW, Held H, Dawson R, Schellnhuber HJ. 2009 Imprecise probability assessment of tipping points in the climate system. *Proc. Natl. Acad. Sci. USA* **106**, 5041–5046.
13. Klose AK, Karle V, Winkelmann R, Donges JF. 2020 Emergence of cascading dynamics in interacting tipping elements of ecology and climate. *R. Soc. Open Sci.* **7**, 200599.
14. Scheffer M, Bascompte J, Brock WA, Brovkin V, Carpenter SR, Dakos V, Held H, Van Nes EH, Rietkerk M, Sugihara G. 2009 Early-warning signals for critical transitions. *Nature* **461**, 53–59.
15. Scheffer M, Carpenter SR, Lenton TM, Bascompte J, Brock W, Dakos V, Van de Koppel J, Van de Leemput IA, Levin SA, Van Nes EH et al.. 2012 Anticipating critical transitions. *Science* **338**, 344–348.
16. Boettiger C, Hastings A. 2013 From patterns to predictions. *Nature* **493**, 157–158.
17. Kinzig AP, Ryan P, Etienne M, Allison H, Elmqvist T, Walker BH. 2006 Resilience and regime shifts: assessing cascading effects. *Ecol. Soc.* **11**, 20.
18. Rocha JC, Peterson G, Bodin Ö, Levin S. 2018 Cascading regime shifts within and across scales. *Science* **362**, 1379–1383.
19. Gao J, Barzel B, Barabási AL. 2016 Universal resilience patterns in complex networks. *Nature* **530**, 307–312.
20. Laurence E, Doyon N, Dubé LJ, Desrosiers P. 2019 Spectral dimension reduction of complex dynamical networks. *Phys. Rev. X* **9**, 011042.
21. Thibeault V, St-Onge G, Dubé LJ, Desrosiers P. 2020 Threefold way to the dimension reduction of dynamics on networks: An application to synchronization. *Phys. Rev. Research* **2**, 043215.
22. Masuda N, Kundu P. 2022 Dimension reduction of dynamical systems on networks with leading and non-leading eigenvectors of adjacency matrices. *Phys. Rev. Research* **4**, 023257.
23. Jiang J, Huang ZG, Seager TP, Lin W, Grebogi C, Hastings A, Lai YC. 2018 Predicting tipping points in mutualistic networks through dimension reduction. *Proc. Natl. Acad. Sci. USA* **115**, E639–E647.
24. Cohen R, Erez K, Ben-Avraham D, Havlin S. 2000 Resilience of the internet to random breakdowns. *Phys. Rev. Lett.* **85**, 4626.
25. Callaway DS, Newman ME, Strogatz SH, Watts DJ. 2000 Network robustness and fragility: Percolation on random graphs. *Phys. Rev. Lett.* **85**, 5468.
26. Cohen R, Erez K, Ben-Avraham D, Havlin S. 2001 Breakdown of the internet under intentional attack. *Phys. Rev. Lett.* **86**, 3682.
27. Newman ME, Strogatz SH, Watts DJ. 2001 Random graphs with arbitrary degree distributions and their applications. *Phys. Rev. E* **64**, 026118.
28. Newman ME. 2002 Spread of epidemic disease on networks. *Phys. Rev. E* **66**, 016128.
29. Pastor-Satorras R, Vespignani A. 2001a Epidemic spreading in scale-free networks. *Phys. Rev. Lett.* **86**, 3200.
30. Pastor-Satorras R, Vespignani A. 2001b Epidemic dynamics and endemic states in complex networks. *Phys. Rev. E* **63**, 066117.
31. Pastor-Satorras R, Vespignani A. 2002 Epidemic dynamics in finite size scale-free networks. *Phys. Rev. E* **65**, 035108.
32. Boguná M, Pastor-Satorras R. 2002 Epidemic spreading in correlated complex networks. *Phys. Rev. E* **66**, 047104.
33. Moreno Y, Pastor-Satorras R, Vespignani A. 2002 Epidemic outbreaks in complex heterogeneous networks. *Euro. Phys. J. B* **26**, 521–529.
34. Masuda N, Konno N. 2006 Multi-state epidemic processes on complex networks. *J. Theor. Biol.* **243**, 64–75.
35. Barrat A, Barthelemy M, Vespignani A. 2008 *Dynamical Processes on Complex Networks*. Cambridge university press.
36. Pastor-Satorras R, Castellano C, Van Mieghem P, Vespignani A. 2015 Epidemic processes in complex networks. *Rev. Mod. Phys.* **87**, 925.
37. Ichinomiya T. 2004 Frequency synchronization in a random oscillator network. *Phys. Rev. E* **70**, 026116.
38. Coutinho B, Goltsev A, Dorogovtsev S, Mendes J. 2013 Kuramoto model with frequency-degree correlations on complex networks. *Phys. Rev. E* **87**, 032106.
39. Kundu P, Khanra P, Hens C, Pal P. 2017 Transition to synchrony in degree-frequency correlated Sakaguchi-Kuramoto model. *Phys. Rev. E* **96**, 052216.
40. Kundu P, Pal P. 2019 Synchronization transition in Sakaguchi-Kuramoto model on complex networks with partial degree-frequency correlation. *Chaos* **29**, 013123.

41. Baronchelli A, Pastor-Satorras R. 2010 Mean-field diffusive dynamics on weighted networks. *Phys. Rev. E* **82**, 011111.
42. Lau HW, Szeto KY. 2010 Asymptotic analysis of first passage time in complex networks. *Europhys. Lett.* **90**, 40005.
43. Antal T, Redner S, Sood V. 2006 Evolutionary dynamics on degree-heterogeneous graphs. *Phys. Rev. Lett.* **96**, 188104.
44. Sood V, Antal T, Redner S. 2008 Voter models on heterogeneous networks. *Phys. Rev. E* **77**, 041121.
45. Masuda N, Konno N. 2006 Networks with dispersed degrees save stable coexistence of species in cyclic competition. *Phys. Rev. E* **74**, 066102.
46. Beisner BE, Haydon DT, Cuddington K. 2003 Alternative stable states in ecology. *Front. Ecol. Environ.* **1**, 376–382.
47. Wunderling N, Stumpf B, Krönke J, Staal A, Tuinenburg OA, Winkelmann R, Donges JF. 2020 How motifs condition critical thresholds for tipping cascades in complex networks: Linking micro-to macro-scales. *Chaos* **30**, 043129.
48. Brummitt CD, Barnett G, D'Souza RM. 2015 Coupled catastrophes: sudden shifts cascade and hop among interdependent systems. *J. R. Soc. Interface* **12**, 20150712.
49. Wunderling N, Donges JF, Kurths J, Winkelmann R. 2021 Interacting tipping elements increase risk of climate domino effects under global warming. *Earth Syst. Dynam.* **12**, 601–619.
50. Wright DG, Stocker TF. 1991 A zonally averaged ocean model for the thermohaline circulation. Part I: Model development and flow dynamics. *J. Phys. Oceanogr.* **21**, 1713–1724.
51. Levermann A, Winkelmann R. 2016 A simple equation for the melt elevation feedback of ice sheets. *Cryosphere* **10**, 1799–1807.
52. Krönke J, Wunderling N, Winkelmann R, Staal A, Stumpf B, Tuinenburg OA, Donges JF. 2020 Dynamics of tipping cascades on complex networks. *Phys. Rev. E* **101**, 042311.
53. Wunderling N, Gelbrecht M, Winkelmann R, Kurths J, Donges JF. 2020 Basin stability and limit cycles in a conceptual model for climate tipping cascades. *New J. Phys.* **22**, 123031.
54. Barabási AL, Albert R. 1999 Emergence of scaling in random networks. *Science* **286**, 509–512.
55. Holme P, Kim BJ. 2002 Growing scale-free networks with tunable clustering. *Phys. Rev. E* **65**, 026107.
56. Newman ME. 2006 Finding community structure in networks using the eigenvectors of matrices. *Phys. Rev. E* **74**, 036104.
57. Kunegis J. 2013 Konect: the koblenz network collection. In *Proceedings of the 22nd International Conference on World Wide Web* pp. 1343–1350.
58. Tu C, Grilli J, Schuessler F, Suweis S. 2017 Collapse of resilience patterns in generalized Lotka-Volterra dynamics and beyond. *Phys. Rev. E* **95**, 062307.
59. Tu C, D'Odorico P, Suweis S. 2021 Dimensionality reduction of complex dynamical systems. *iScience* **24**, 101912.
60. Kundu P, Kori H, Masuda N. 2022 Accuracy of a one-dimensional reduction of dynamical systems on networks. *Phys. Rev. E* **105**, 024305.
61. Schoch D. 2022 *networkdata: Repository of Network Datasets*. R package version 0.1.10.
62. Silvis A, Kniowski AB, Gehrt SD, Ford WM. 2014 Roosting and foraging social structure of the endangered Indiana bat (Myotis sodalis). *PLoS ONE* **9**, e96937.
63. Lusseau D, Schneider K, Boisseau OJ, Haase P, Slooten E, Dawson SM. 2003 The bottlenose dolphin community of Doubtful Sound features a large proportion of long-lasting associations. *Behav. Ecol. Sociobiol.* **54**, 396–405.
64. Weeks MR, Clair S, Borgatti SP, Radda K, Schensul JJ. 2002 Social networks of drug users in high-risk sites: Finding the connections. *AIDS and Behavior* **6**, 193–206.
65. Casey C, Charrier I, Mathevon N, Reichmuth C. 2015 Rival assessment among northern elephant seals: evidence of associative learning during male–male contests. *R. Soc. Open Sci.* **2**, 150228.
66. Freeman LC, Webster CM, Kirke DM. 1998 Exploring social structure using dynamic three-dimensional color images. *Soc. Netw.* **20**, 109–118.
67. Coleman JS. 1964 *Introduction to Mathematical Sociology*. New York: Free Press.
68. Adelman JS, Moyers SC, Farine DR, Hawley DM. 2015 Feeder use predicts both acquisition and transmission of a contagious pathogen in a North American songbird. *Proc. R. Soc. B* **282**, 20151429.
69. Gleiser PM, Danon L. 2003 Community structure in jazz. *Adv. Complex Syst.* **6**, 565–573.

70. Zachary WW. 1977 An information flow model for conflict and fission in small groups. *J. Anthropol. Res.* **33**, 452–473.
71. Bull CM, Godfrey S, Gordon D. 2012 Social networks and the spread of Salmonella in a sleepy lizard population. *Mol. Ecol.* **21**, 4386–4392.
72. Firth JA, Sheldon BC. 2015 Experimental manipulation of avian social structure reveals segregation is carried over across contexts. *Proc. R. Soc. B* **282**, 20142350.
73. Newman ME. 2006 Finding community structure in networks using the eigenvectors of matrices. *Phys. Rev. E* **74**, 036104.
74. Gill P, Lee J, Rethemeyer KR, Horgan J, Asal V. 2014 Lethal connections: The determinants of network connections in the Provisional Irish Republican Army, 1970–1998. *Intl. Interact.* **40**, 52–78.
75. Freeman LC, Freeman SC, Michaelson AG. 1988 On human social intelligence. *J. Soc. Biol. Struct.* **11**, 415–425.
76. Sah P, Nussear KE, Esque TC, Aiello CM, Hudson PJ, Bansal S. 2016 Inferring social structure and its drivers from refuge use in the desert tortoise, a relatively solitary species. *Behav. Ecol. Sociobiol.* **70**, 1277–1289.
77. Davis S, Abbasi B, Shah S, Telfer S, Begon M. 2015 Spatial analyses of wildlife contact networks. *J. R. Soc. Interface* **12**, 20141004.
78. van Dijk RE, Kaden JC, Argüelles-Ticó A, Dawson DA, Burke T, Hatchwell BJ. 2014 Cooperative investment in public goods is kin directed in communal nests of social birds. *Ecol. Lett.* **17**, 1141–1148.
79. van de Leemput IA, van Nes EH, Scheffer M. 2015 Resilience of alternative states in spatially extended ecosystem. *PLoS ONE* **10**, e0116859.
80. Bel G, Hagberg A, Meron E. 2012 Gradual regime shifts in spatially extended ecosystems. *Theo. Ecol.* **5**, 591–604.
81. Lovejoy TE, Nobre C. 2018 Amazon tipping point. *Sci. Adv.* **4**, eaat2340.
82. Kouvaris NE, Kori H, Mikhailov AS. 2012 Traveling and pinned fronts in bistable reaction-diffusion systems on networks. *PLoS ONE* **7**, e45029.
83. Kouvaris NE, Mikhailov AS. 2013 Feedback-induced stationary localized patterns in networks of diffusively coupled bistable elements. *Europhys. Lett.* **102**, 16003.
84. Yang T, Zhang C, Han Q, Zeng CH, Wang H, Tian D, Long F. 2014 Noises-and delay-enhanced stability in a bistable dynamical system describing chemical reaction. *Eur. Phys. J. B* **87**, 1–11.